Microporous and Mesoporous Materials 142 (2011) 236–244

Contents lists available at ScienceDirect

Microporous and Mesoporous Materials

journal homepage: www.elsevier.com/locate/micromeso

Dynamics of water diffusion in mesoporous zeolites

Rustem Valiullin [a], Jörg Kärger [a,*], Kanghee Cho [b,c], Minkee Choi [b], Ryong Ryoo [b,c]

[a] Faculty of Physics and Earth Science, University of Leipzig, Linnèstr. 5, D-04103 Leipzig, Germany
[b] Center for Functional Nanomaterials, Department of Chemistry, KAIST, Daejeon 305-701, Republic of Korea
[c] Graduate School of Nanoscience and Technology (WCU), KAIST, Daejeon 305-701, Republic of Korea

ARTICLE INFO

Article history:
Received 29 June 2010
Received in revised form 29 November 2010
Accepted 5 December 2010
Available online 10 December 2010

Keywords:
LTA
BEA
Mesoporous Zeolites
Diffusion
Water

ABSTRACT

Pulsed field gradient NMR has been applied to investigate water diffusion in Na^+-form zeolites beta and LTA if, in addition to the micropores, the intracrystalline space is traversed by a network of mesopores. In zeolite beta, the presence of the mesopores is found to enhance the rate of molecular diffusion by a factor of 3. The measurements with mesoporous zeolite LTA yield diffusivities which reproduce the order of magnitude of the diffusivities found in previous studies with genuine microporous specimens.

1. Introduction

The use of microporous materials in mass separation and shape-selective catalysis results from the intimate contact of the guest molecules with the host surface [1]. This, in general, is brought about by choosing a pore size as close to the molecular dimension as possible. This closeness, however, has to be purchased by small transport rates of the guest molecules in the host system which, in turn, may notably reduce the performance of microporous materials in their technological application. This limitation may be circumvented by the application of materials with hierarchically organized pore systems [2–7] where molecular exchange between ranges of microporosity with the crystal surroundings is accelerated by a hierarchical pore connectivity of micropores and mesopores (or even macropores) traversing the intracrystalline space. Until now, few works have been devoted to generate such meso/micropore structure in the zeolite crystal through hard templating [8–10], or supramolecular soft-templating [3,11–13] methods, and post-synthetic dealumination or desilication [14–17]. Of these routes, the synthesis method that uses quaternary ammonium-type cationic organosilane surfactant (OS) as the mesopore-generating agent has attracted much attention as easy one-pot hydrothermal method [3,4,18,19]. Also, this method has the advantage of controlling mesopore diameter and volume according to the size and the amount of OS.

Recently, Cho et al. reported that mesoporous LTA zeolite synthesized by using OS exhibited more than hundred times rapid xenon uptake in comparison with solely microporous LTA [19]. The enhanced molecular transport was directly evidenced by ^{129}Xe NMR technique and volumetric adsorption at room temperature. Also, there have been other reports which showed the effects of meso/micropore structure on molecular diffusion in zeolites. Christensen et al. reported that a hierarchical MFI zeolite, which was synthesized in a nano-carbon template, adsorbed isobutene gas significantly faster than conventional MFI zeolite [20]. Groen et al. measured the rate of neo-pentane uptake by a desilicated MFI zeolite, and reported that the adsorption rate was increased to about 100 times, in comparison with conventional MFI zeolite [21]. Liu et al. used hyperpolarized ^{129}Xe NMR spectroscopy to investigate xenon exchange between mesopores and micropores in a starch-templated MFI zeolite [22]. They reported that xenon exchange between the two kinds of pore systems occurred rapidly in the NMR time scale, using a variable-temperature NMR experiment and 2D exchange spectroscopy.

Being directly sensitive to the rate of molecular displacements over micrometers during observation times of milliseconds till seconds, the pulsed field gradient technique of NMR (PFG NMR) [23–25] has proved to be a particularly versatile tool for studying the translational dynamics of guest molecules in porous materials [26], in particular in zeolites [27]. In the present study, these potentials have been exploited for the investigation of water diffusion in Na^+-form BEA and LTA zeolites containing a hierarchical micro- and mesopore architecture, which were synthesized by using OS.

* Corresponding author. Tel.: +49 341 9732502; fax: +49 341 9732549.
E-mail address: kaerger@physik.uni-leipzig.de (J. Kärger).

1387-1811/$ - see front matter © 2010 Elsevier Inc. All rights reserved.
doi:10.1016/j.micromeso.2010.12.005

2. Experimental

2.1. Materials synthesis and characterization

The hydrothermal syntheses of BEA and LTA zeolites were performed with adding an OS (see Table 1, footnote e, for molecular structure) as the mesopore-generating agent into conventional synthetic compositions. In the syntheses of BEA zeolites, sodium silicate (Na_2O 17 wt.%, SiO_2 29 wt.%, aqueous solution), sodium aluminate (Na_2O 53.0 wt.%, Al_2O_3 42.5 wt.%), tetraethylammonium hydroxide (40 wt.% aqueous solution, denoted by 'TEAOH'), sodium hydroxide and OS (49.6 wt.% solution in methanol) were homogeneously dissolved in distilled water. The molar composition of the initial synthetic mixture was $100SiO_2/1.95Al_2O_3/54TEAOH/5Na_2O/4900H_2O/n$ OS (n = 0, 2 or 5). The synthetic mixture was heated for 10 days at 403 K inside a tumbled autoclave. The product was filtered, washed by distilled water, dried at 373 K and calcined at 823 K. The obtained BEA zeolite samples are denoted by 'Na-BEA-n'. Here, 'Na' means the Na^+-containing synthesis condition of the BEA zeolite, and the numbers following 'BEA' refer to the number of OS moles (n) used for the gel composition. According to the elemental analysis using inductively coupled plasma atomic emission spectroscopy, the BEA zeolite products exist approximately in the 90% H^+–10% Na^+ form. The synthesis of LTA zeolite was performed as reported elsewhere [19], except for the difference in the amount of OS. All zeolite products are prepared in the Na^+ form. Thus obtained LTA zeolite samples are denoted by 'Na-LTA-n'. Characterization of the zeolite samples was performed with XRD, SEM, and N_2 sorption analysis as described in Ref. [19]. Additionally, Ar and water sorption analyses were carried out for Na-LTA zeolite samples. Ar sorption isotherms were volumetrically measured at the temperature of liquid Ar (87 K) using a Micromeritics ASAP 2020 instrument. Water sorption isotherms were measured at 300 K using gravimetric analysis system which was equipped with a magnetic suspension microbalance (Rubotherm). Before the adsorption measurements, three Na-LTA zeolite samples were outgassed for 3 h at 573 K under 10^{-4} Pa.

2.2. PFG NMR diffusion measurements

The PFG NMR technique is able to determine the probability distribution $P(z,t)$ (the "propagator") of molecular displacements of typically micrometers in the direction of the applied field gradients over an observation time of milliseconds till seconds. In general, PFG NMR measurements are performed under equilibrium conditions, reflecting the rate of molecular re-distribution within the system under study. $P(z,t)$ results as the Fourier transform of the primary quantity, the PFG NMR signal attenuation $S(q,t)$, which is directly accessible by the experiments [26,28]. The quantity q is the product $q = \gamma\delta g$ of the gyromagnetic ratio (for protons, $\gamma = 2.67 \times 10^8\ T^{-1}\ s^{-1}$) and the width ($\delta$) and amplitude ($g$) of the gradient pulses. It is referred to as the generalized scattering vector.

Analysis is particularly straightforward if, with respect to the considered space and time scales, the system under study may be considered to be homogeneous and isotropic. In this case, molecular diffusion follows Fick's 1st law and the propagator may be easily shown to be represented by a Gaussian with the mean square width (molecular mean square displacement) given by the Einstein relation [26,28,29].

$$\langle r^2(t)\rangle = 6Dt \tag{1}$$

During observation time t, with D denoting the coefficient of self-diffusion also referred to as the (self-) diffusivity. In this case, the PFG NMR attenuation curve follows a simple exponential dependence

$$S(q,t) = \exp(-q^2Dt) \equiv \exp(-q^2\langle r^2(t)\rangle/6) \tag{2}$$

In PFG NMR diffusion measurements with nanoporous particles of finite size, just like zeolite crystallites, the situation is often more complicated. With increasing "observation" time t more and more molecules will leave their crystallites, so that only a certain fraction $p(t)$ of the molecules will have remained in one and the same crystallite over the total observation time. In this case, the PFG NMR attenuation curve may be approached by the sum of two exponentials.

Table 1
Pore textural properties of LTA and BEA zeolites synthesized with various amounts of organosilane surfactant.

Sample	n[e]	S_{BET}[f] ($m^2\ g^{-1}$)	V_{tot}[g] (mL g^{-1})	V_{micro}[h] (mL g^{-1})	V_{meso}[i] (mL g^{-1})
Na-LTA-0[a]	0	13	0.01	N.D.[j]	N.D.[j]
Na-LTA-2[a]	2	45	0.09	N.D.[j]	N.D.[j]
Na-LTA-5[a]	5	86	0.20	N.D.[j]	N.D.[j]
Na-LTA-0[b]	0	N.D.[j]	N.D.[j]	N.D.[j]	N.D.[j]
Na-LTA-2[b]	2	496	0.34	0.11	0.23
Na-LTA-5[b]	5	525	0.51	0.11	0.4
Ca-LTA-0[c]	0	475	0.23	0.21	0.02
Ca-LTA-2[c]	2	541	0.36	0.21	0.15
Ca-LTA-5[c]	5	599	0.55	0.20	0.35
Na-BEA-0[d]	0	530	0.34	0.16	0.18
Na-BEA-2[d]	2	580	0.45	0.16	0.29
Na-BEA-5[d]	5	587	0.56	0.17	0.39

[a] The porosity of Na-LTA zeolites measured from N_2 adsorption isotherm at 77 K.
[b] The microporosity of Na-LTA zeolites could not be measured from N_2 adsorption isotherm at 77 K because of too slow N_2 uptake into micropores of Na-LTA zeolite in equilibration time scale of sorption analyzer. Therefore, the pore textural properties of Na-LTA zeolites were measured from Ar adsorption isotherms at 87 K.
[c] LTA zeolite samples which were ion-exchanged by Ca^{2+} ion were designated by Ca-LTA-n. Ca^{2+} ion exchange is known to increase the α-cage (micropore) aperture enough for rapid uptake of N_2 molecules into LTA zeolite frameworks. The pore textural properties of Ca-LTA zeolites could be measured from N_2 adsorption isotherms at 77 K.
[d] The porosity of Na-BEA zeolites measured from N_2 adsorption isotherm at 77 K.
[e] n is the number of organosilane moles in synthesis composition. The synthesis composition is $100SiO_2/333Na_2O/67.0Al_2O_3/20{,}000H_2O/n\ (CH_3O)_3SiC_3H_6N(CH_3)_2C_{16}H_{33}$ for LTA, and $100SiO_2/1.95Al_2O_3/54TEAOH/5Na_2O/4900H_2O/n\ (CH_3O)_3SiC_3H_6N(CH_3)_2C_3H_6N(CH_3)_2C_3H_6$ for BEA.
[f] S_{BET}, BET surface area obtained from N_2 or Ar adsorption isotherm in the relative pressure range of 0.05–0.20.
[g] V_{tot}, total pore volume was derived at $P/P_0 = 0.97$.
[h] V_{micro}, micoropore volume was calculated from the t-plot method.
[i] V_{meso}, mesopore volume was calculated as the difference between V_{tot} and V_{micro}.
[j] Not determined. Data are not given explicitly.

$$S(q,t) = p(t)\exp\left(-q^2\langle r^2(t)\rangle_{\text{intra}}/6\right) + [1-p(t)] \times \exp\left(-q^2\langle r^2(t)\rangle_{\text{long-range}}/6\right) \quad (3)$$

Determination of the function $p(t)$ for different observation times provides direct evidence on the rate of molecular exchange between the different crystallites. Exactly the same information, however, over much larger space and time scales are provided by conventional tracer exchange experiments. This way of analysis of PFG NMR data has therefore been referred to as NMR tracer desorption [27,30].

As a key quantity of these studies, one may determine the so-called first statistical moment of the tracer exchange curve via the relation [27,30,31].

$$M_1 \equiv \tau_{\text{intra}} = \int_0^\infty p(t)\mathrm{d}t \quad (4)$$

The first statistical moment M_1 coincides with the intracrystalline mean life time. This may be easily rationalized by considering the approach $p(t) \sim \exp(-t/\tau)$ from which, via Eq. (4), the intracrystalline mean life time τ_{intra} is identified as the time constant τ of the exponential.

For an assessment of the PFG NMR data it is important to rationalize the information contained in the mean square displacements appearing in Eqs. (2) and (3). For an assessment of $\langle r^2(t)\rangle_{\text{intra}}$ it is essential to have in mind that the mean value of the squared displacements within a crystal is confined by the crystal size, yielding a maximum value of

$$D_{\text{restr.}} = \frac{R^2}{5t} \quad (5)$$

where the crystal is approached by a sphere of radius R. PFG NMR studies of intracrystalline diffusion are thus yielding an intracrystalline mean square displacement $\langle r^2(t)\rangle_{\text{intra}}$ which coincides with the prediction of the Einstein relation, Eq. (1), $\langle r^2(t)\rangle_{\text{intra}} = 6Dt$ for sufficiently small displacement, i.e., small observation times and which, with increasing time, eventually approaches the limiting value as given by Eq. (5). For mesoporous zeolites, i.e., for micropore spaces traversed by mesopores, the intracrystalline mean square displacement may be noted in the form

$$\langle r^2(t)\rangle_{\text{intra}} = \langle r^2(t)\rangle_{\text{micro}} + \langle r^2(t)\rangle_{\text{meso}} \quad (6)$$

where $\langle r^2(t)\rangle_{\text{micro}}$ and $\langle r^2(t)\rangle_{\text{meso}}$ denote, respectively, the mean squared total displacements in the micro and mesopores during the observation time t. As a consequence of the mutual interpenetration of the networks of micro and mesopores, the respective molecular displacements are independent from each other so that, in Eq. (6), cross terms of the type $\langle r(t)_{\text{micro}}\, r(t)_{\text{meso}}\rangle$ vanish. Considering dynamic equilibrium between micro and mesopores one may note

$$t_{\text{micro}}/t_{\text{meso}} = p_{\text{micro}}/p_{\text{meso}} \quad (7)$$

where $t_{\text{micro(meso)}}$ and $p_{\text{micro(meso)}}$ denote, respectively, the total time (during observation time t) and the relative amount of molecules in the micro(meso)pores. Combining Eqs. (6) and (7), by use of Eq. (1) one finally obtains

$$D_{\text{intra}} = p_{\text{micro}}D_{\text{micro}} + p_{\text{meso}}D_{\text{meso}} \quad (8)$$

Correspondingly, one has for displacements through the bed of zeolite crystallites

$$\langle r^2(t)\rangle_{\text{long-range}} = \langle r^2(t)\rangle_{\text{intra}} + \langle r^2(t)\rangle_{\text{inter}} \quad (9)$$

where the subscripts now refer to displacements in the crystal interior and the intercrystalline space. By the same reasoning as used for deriving equation (8) and with the corresponding notation, we do now obtain

$$D_{\text{long-range}} = \frac{\langle r^2(t)\rangle_{\text{intra}}}{6t} + p_{\text{inter}}D_{\text{inter}} \quad (10)$$

where, in addition, we have made use of the relations $p_{\text{inter}} \ll p_{\text{intra}}$ (i.e. $t_{\text{intra}} \approx t$ and, since $p_{\text{inter}} + p_{\text{intra}} = 1$, $p_{\text{intra}} \approx 1$). For molecular displacements notably exceeding the crystal sizes (as a prerequisite of the measurement of long-range diffusion), the first term on the right-hand side may be shown to be notably exceeded by the second term [39,47] leading to

$$D_{\text{long-range}} = p_{\text{inter}}D_{\text{inter}} \quad (11)$$

As a general requirement of all diffusion studies by PFG NMR, the signal intensity must be large enough to ensure a reliable determination of its attenuation and hence, via Eqs. (2) and (3), respectively, of the molecular displacements. This means, in particular, that for any system there is a certain lower temperature limit for the range of measurement. This limit is mainly determined by the transverse nuclear magnetic relaxation time which decreases with decreasing temperature and, eventually, prohibits the application of field gradients of sufficiently large intensities q [23–27].

Prior to the PFG NMR measurements, the zeolite material was introduced into sample tubes of 7.5 mm outer diameter, to a filling height of 10 mm. Under continuous evacuation, these tubes were heated at a rate of 10 K h^{-1} to 673 K. After keeping them at this temperature for about 12 h and cooling down, under continued evacuation, the guest molecules (water) were introduced by means of liquid nitrogen from a calibrated volume under a well-defined pressure. Subsequently, the sample tubes were closed hermetically. Equilibration of the guest molecules within the sample was confirmed by a repetition of the measurements over a time span of several weeks, which yielded completely coinciding results. The volumes of the water bulk phase corresponding to the amounts adsorbed were chosen to coincide with the total pore volumes determined by N_2 adsorption as presented in Table 1. For the Na-LTA-0 sample which was synthesized without OS, the signal intensities brought about by the amount adsorbed turned out to be insufficient so that this sample had to be left out of our considerations.

In addition to its omnipresence in technological application, the use of water as a guest molecule was in particular motivated by the fact that, among the proton-containing molecules, it is the only one for which, as a consequence of the above indicated limitations, PFG NMR may be applied to diffusion studies in the micropores of both types of zeolites considered in this study. All diffusion measurements have been performed by means of the home-built PFG NMR spectrometer FEGRIS 400 operating at a ^{1}H resonance frequency of 400 MHz, with a maximum gradient amplitude of 35 T m^{-1} [32,33]. Application of the stimulated-echo technique [23–25] allowed a variation of the observation time from 2 to 10 ms.

3. Results and discussion

3.1. Host systems under study

Characterization results of BEA and LTA zeolites from SEM investigation and sorption analysis were summarized in Figs. 1 and 2. Table 1 provides a survey of the quantitative analysis of the adsorption data. The SEM images for Na-BEA zeolites in Fig. 1a show similar particle morphologies for all three zeolite samples synthesized under the presence or absence of OS. The zeolite particle diameters were approximately in the range of 200 nm–1 μm, exhibiting very high surface roughness in the 50-nm or smaller nanoscale. Fig. 1b and c reports N_2 adsorption isotherms and corresponding pore-diameter distributions of the Na-BEA

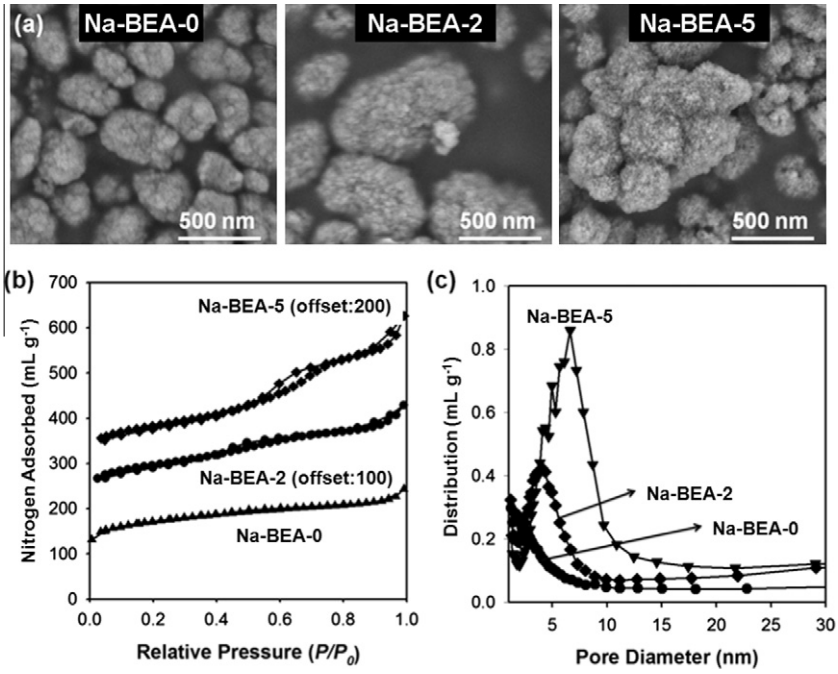

Fig. 1. (a) SEM images of Na-BEA zeolite samples with different mesoporosity, (b) N_2 adsorption isotherms of Na-BEA zeolite samples at 77 K and (c) corresponding BJH mesopore size distributions.

zeolites. This adsorption data shows that the Na-BEA-0 zeolite sample contained very little mesoporosity as compared to Na-BEA-2 and Na-BEA-5.

The SEM images for LTA zeolites are shown in Fig. 2a. The SEM images are essentially the same as reported in [19]; the surface roughness increased with the OS content in gel composition. Cho et al. analyzed the surface structure using high-resolution SEM to clarify that the surface roughness was due to formation of intracrystalline mesoporous channels with a narrow distribution of diameters [34]. In Fig. 2b, N_2 sorption isotherms of Na-LTA zeolite samples showed no adsorption of nitrogen at low relative pressure ($P/P_0 < 0.02$), indicating that N_2 molecules scarcely diffused into micropores of LTA zeolite in the equilibration time scale of the sorption analyzer [35]. Slow uptake of nitrogen was attributed to tight micropore apertures (4.2 Å) of the Na-LTA zeolite for N_2 molecules (kinetic diameter = 4.4 Å, [36]). Therefore, the adsorbate was replaced by Ar with smaller molecular size (kinetic diameter = 3.9 Å). The Ar sorption results of Na-LTA zeolites containing mesoporosity (i.e., Na-LTA-2 and Na-LTA-5) exhibited micropore filling of Ar atom (i.e., the adsorption increase in the region $P/P_0 < 0.02$) as well as capillary condensation in mesopores (Fig. 2c). On the other hand, the Ar adsorption isotherm for Na-LTA-0 (the LTA sample which was synthesized by the synthesis procedure without OS) showed very little adsorption into micropores. This result for Ar sorption indicated that the molecular diffusion into the Na-LTA zeolite was significantly enhanced by the generation of mesopores. However, the uptake rate into small micropores was still too slow to reach equilibrium within the given equilibration time (30 min at each point) in the case of the Na-LTA-0 zeolite. Hence, for the measurement of microporosity in LTA zeolite samples, the Na-LTA zeolites were fully ion-exchanged by Ca^{2+}. The LTA zeolite samples which were fully ion-exchanged by Ca^{2+} were denoted by 'Ca-LTA-*n*'. The Ca^{2+} ion exchange is known to increase the α-cage aperture to 0.48 nm [19]. N_2 sorption isotherms of Ca-LTA zeolites confirmed that the LTA zeolite samples had approximately the same amount of microporosity, regardless of the OS content in synthesis composition (Fig. 2d). However, the mesoporosity of the samples gradually increased with respect to the amount of used OS.

Water (kinetic diameter = 2.8 Å, [36]) adsorption by the Na-LTA zeolites occurred quite rapidly at 300 K, requiring an equilibration time less than 5 min at each relative pressure. The adsorption isotherms in Fig. 3 show that mesoporous Na-LTA zeolites (i.e., Na-LTA-2 and Na-LTA-5) had a very small amount of adsorption due to micropores as compared with the solely microporous Na-LTA zeolite (Na-LTA-0, see also Table 1). The water adsorption, corresponding to $P/P_0 < 0.02$, decreased against the increase in mesoporosity. This result is quite surprising whereas Ca-LTA zeolite samples exhibited very similar adsorption capacities due to micropore filling in the case of N_2 adsorption. As judged from the difference between water and N_2 adsorption, the mesoporous zeolite samples were more hydrophobic than the solely microporous Na-LTA-0 zeolite. The hydrophobicity may be suggested as a result of Si–C bonds, which could remain on the mesopore walls after calcination at 823 K (see the OS molecular structure in Table 1). No carbon black formation was detectable by eyes. Nevertheless, elemental analysis of the freshly calcined LTA samples showed the C/Si molar ratios of 0.078 for Na-LTA-2, and C/Si = 0.086 for Na-LTA-5. Such carbon content could make the mesoporous LTA zeolite samples somewhat hydrophobic if the carbon existed as in Si–C bonds at the surface of the mesopore walls.

3.2. Water diffusion in mesoporous Na-BEA

Over the whole temperature range considered (−20 to 100 °C), the PFG NMR signal attenuation curves were found to be mono-exponential, following the dependence of Eq. (2). Fig. 4 provides a summary of the resulting diffusivities. For comparison, also the diffusivity data for bulk water [37] and the coefficients of intracrystalline diffusion of water in zeolite NaX [38] are presented. Via Eq. (1), the mean diffusion paths covered in the present experiments were found to range from about 0.6 to 10 μm. The magnitude of these displacements notably exceeded the extension of the individual zeolite particles as shown by Fig. 1a.

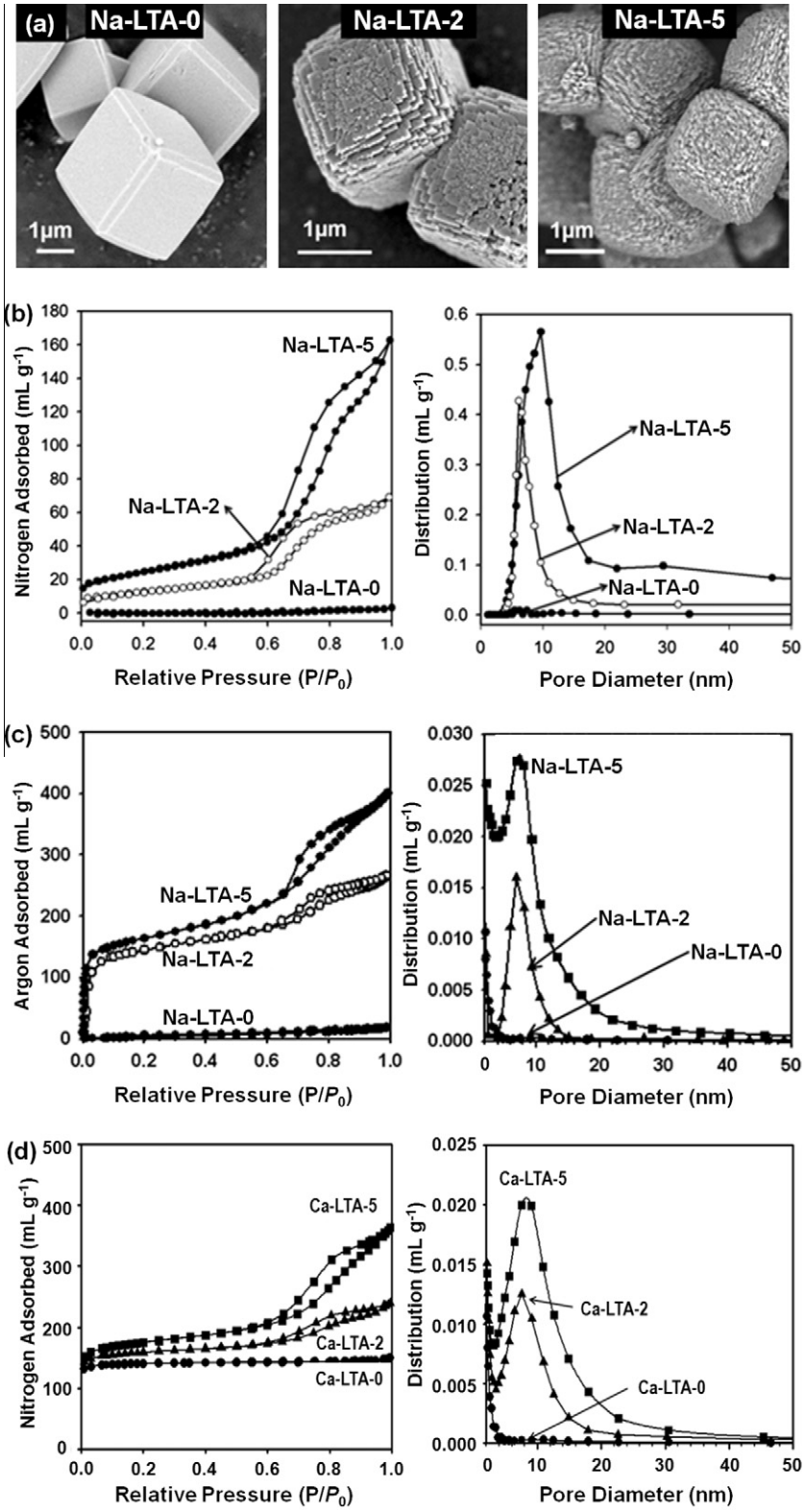

Fig. 2. (a) SEM images of Na-LTA zeolite samples with different mesoporosity, (b) N_2 adsorption isotherms of the Na-LTA zeolite samples at 77 K and corresponding BJH mesopore size distributions and (c) Ar adsorption isotherms at 87 K and corresponding BJH mesopore size distributions, and (d) N_2 adsorption isotherms of Ca-LTA zeolite samples at 77 K and BJH mesopores size distributions. Ca^{2+} ion exchange is known to increase the α-cage (micropore) aperture enough for rapid uptake of N_2 molecules into LTA zeolite frameworks.

For beds of zeolite crystallites, diffusion measurements performed under such conditions are known to yield the long-range diffusivity [27,39] which results as the product of the relative number p_{inter} of molecules in the intercrystalline space and their diffusivity D_{inter} (Eq. (11)). If the rate of mutual collisions of the molecules in the intercrystalline space is much smaller than the

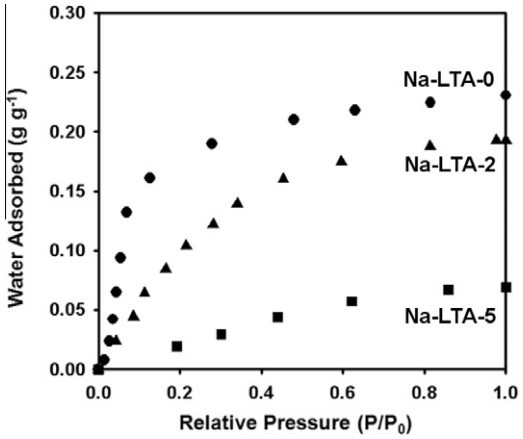

Fig. 3. Water adsorption isotherms of Na-LTA zeolite samples at 300 K which were measured by using gravimetric analysis system.

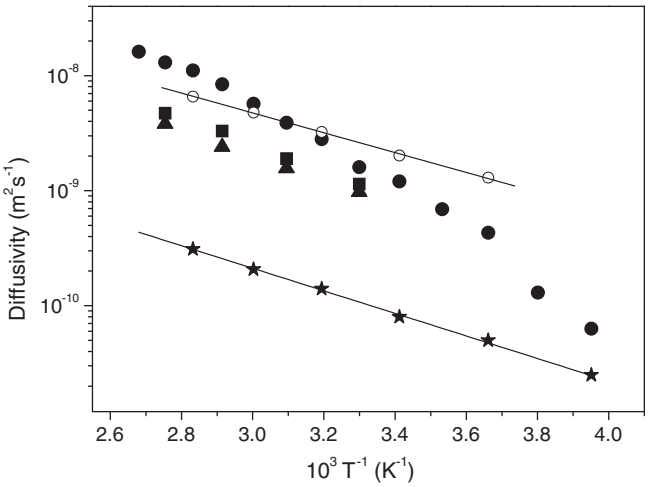

Fig. 4. Arrhenius plot of diffusivities of water in Na-BEA-0 (triangles), Na-BEA-2 (squares) and Na-BEA-5 (filled circles). For comparison, diffusivities of bulk water (open circles, line shows fit of the Arrhenius equation to the data with E_A = 16.5 kJ mol^{-1}) and water in NaX zeolite (stars, line shows fit of the Arrhenius equation to the data with E_A = 18.7 kJ mol^{-1}).

rate of collisions with the pore wall (which may be implied in the present study), the temperature dependence of the effective diffusivity is essentially given by p_{inter}. Since p_{inter} is proportional to the guest pressure in the surrounding atmosphere, it follows an Arrhenius dependence with the isosteric heat of adsorption as the relevant activation energy.

For zeolites in the Na^+-form, the heat of water adsorption and, correspondingly, the activation energy of long-range diffusion (≈60 kJ mol^{-1}) [40] notably exceed the activation energies observed in the present study (≈20–30 kJ mol^{-1}). The observed displacements should result, therefore, from molecular trajectories on which the water molecules remain in intimate contact with the matrix of the host materials. This might be brought about by "bridges" between the different particles and/or large areas of intimate mutual contact. The energy differences to be overcome on such diffusion paths may be estimated to be ≈22 kJ mol^{-1}, as resulting as the activation energy from the experimental diffusivity data in the medium-temperature region from about 300 K to 360 K.

For an assessment of the observed diffusivities, Fig. 4 as well contains literature data on the diffusivity in bulk water [37] and on the intracrystalline diffusivity of water in zeolite NaX [38,41]. The activation energies of water diffusion in NaX, Na-BEA-0 and Na-BEA-2 zeolites were found to be close to that in the bulk fluid, indicating a similar strength in the binding energies of the water molecules with the other water molecules and with the sodium cations. At sufficiently high temperatures, the activation energy in Na-BEA-5 was also close to this value. The sequence in the magnitude of the diffusivities reflects the expected behaviour: the rate of diffusion increases with the increase of pore space in the host system.

In Na-BEA-5, the diffusivities perceptibly deviated from an Arrhenius dependency and became smaller with decreasing temperature. Such behaviour may be referred to the existence of additional transport resistances which become progressively relevant with decreasing temperatures. On the basis of the given data, a specification of the mechanisms giving rise to this behaviour is not possible. In the temperature range below the water freezing point, however, the observed behaviour might be easily referred to the onset of freezing in the free space between the particles and, eventually, in the mesopores. These frozen regions were supposed to serve as the additional obstacles progressively impeding the propagation within the (remaining) fluid phase. In [42], this process has even been found to give rise to an effect of hysteresis in comparison with the diffusion properties of the sample on the melting and freezing branches.

Most remarkably, for sufficiently low temperatures (i.e., for a sufficiently large amount of blockages for the remaining fluid molecules), the water diffusivity in Na-BEA-5 was found to drop to the values for intracrystalline diffusion in zeolite NaX. At sufficiently high temperatures, on the other hand, it approached the diffusivity in bulk water. PFG NMR diffusion measurements with zeolites Na-BEA-0 and Na-BEA-2 at similarly low temperatures were prohibited by the rapidly decaying transverse nuclear magnetic relaxation time in these samples.

It is important to emphasize that, with diffusion path lengths notably exceeding the size of the individual crystallites, it is the influence of the mesoporosity on long-range rather than on intracrystalline diffusion which is explored by the present studies. With Eq. (11), variation in the long-range diffusivities is seen to be possibly caused by both a variation in the relative amount p_{inter} of molecules in the intercrystalline space and in the intercrystalline diffusivity D_{inter}, with the latter quantity depending on both the geometry of the intercrystalline space. With the presently available data it would be rather speculative to decide which of these influences gives rise to the observed sequence of the diffusivities as reflected by Fig. 4.

3.3. Water diffusion in mesoporous Na-LTA zeolite

In striking contrast with BEA zeolite specimens, the PFG NMR attenuation curves for water diffusion in Na-LTA-2 exhibit a pronounced deviation from a mono-exponential dependence. As an example, Fig. 5 shows the attenuation curves observed at 50 °C as a function of the observation time t. Following Eq. (3), the attenuation curves can be approached by a superposition of two exponentials, where the slope of the second, less steeply decaying one is known to provide information about the intracrystalline diffusivity [44–46]. It turned out, however, that, as a consequence of the scattering in the attenuation data, in particular for large observation times t and large gradient intensity values q^2t, a reliable fitting procedure necessitates some further assumption. As a first-order approximation, we have therefore chosen to represent the value of $\langle r^2(t)\rangle_{intra}$ by its maximum value, as following by inserting $D_{restr.}$ (Eq. (5) into Eq. (1)). Fig. 6 displays the relative contribution $p(t)$ of the thus resulting, slowly decaying component as a function of the observation time, together with the corresponding quantities for

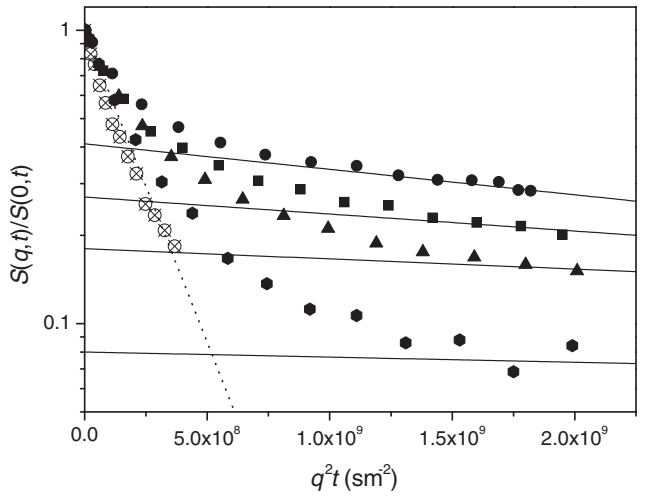

Fig. 5. Spin-echo diffusion attenuation functions for water in the Na-LTA-2 sample measured at 50 °C at different diffusion times of 2 ms (circles), 3 ms (squares), 5 ms (triangles) and 10 ms (diamonds). The solid lines show the slow diffusing components, approached by equating the effective diffusivity with the limiting value as given by $D_{restr.}$ (Eq. (5)). The dotted line is fit of Eq. (2) to the experimental data at low-q limit with the diffusivity $D_{long\text{-}range} = 4.9 \times 10^{-9}$ m^2 s^{-1}. The crossed circles show diffusion attenuation for the sample Na-LTA-5 measured at 2 ms diffusion time.

40, 50 and 60 °C. These curves have been referred to as the NMR tracer desorption curves [27,30]. For an estimate of the intracrystalline mean life times, the curves have been approached by exponentials. The resulting time constants (i.e., the intracrystalline mean life time, τ_{intra}) are indicated in the insert.

Under the conditions of diffusion limitation, the intracrystalline mean life time is correlated with the intracrystalline diffusivity D_{intra} by the relation [31,39]

$$D_{intra} = R^2/(15\tau_{intra}) \quad (12)$$

where, once again, the crystal has been approached by a sphere of radius R. In turn, the right-hand side of Eq. (12) may be considered as the definition of an effective diffusivity ($D_{intra,tracer\text{-}desorption}$) which would result by considering the time constant in classical tracer exchange experiment. Since, in addition to the influence of intracrystalline diffusion, intracrystalline life time may be further enhanced by possibly existing surface resistances [48], $D_{intra,tracer\text{-}desorption}$ represents a lower limit of the (genuine) intracrystalline diffusivity.

Fig. 7 displays these values for water in the mesoporous Na-LTA zeolite under study (where a mean crystal radius of $R \approx 2$ μm has been implied). Also included are the literature data for water diffusion in solely microporous LTA zeolite [39,43]. For comparison, also the maximum value of $D_{restr.}$, following from Eq. (5) with $t = 2$ ms, is indicated. With Fig. 5, the PFG NMR attenuation curves are found to be nicely approached with intracrystalline mean square displacements as following from Eq. (5), i.e., by assuming the limiting case of restricted diffusion. Under such conditions, the genuine (i.e., unrestricted) intracrystalline diffusivity can immediately be concluded to exceed the value of $D_{restr.}$. Not unexpectedly, water diffusion in Na-LTA-2 is thus found to definitely exceed the diffusivity in solely microporous Na-LTA. With Eq. (8), this finding may be formulated by the following inequality.

$$D_{micro} < p_{micro}D_{micro} + p_{meso}D_{meso} \quad (13)$$

where we have equated the diffusivities in the micropore spaces of solely microporous and Na-LTA-2. By considering the normalization condition $p_{micro} + p_{meso} = 1$, this inequality is seen to be equivalent with the inequality $D_{micro} < D_{meso}$, i.e. the fact that molecular propagation in the mesopores occurs at higher rates than in the micropores. Since, under the given conditions, PFG NMR is only able to provide a lower limit of D_{intra}, it is impossible to further specify this enhancement. It is important to note that, though being of a similar order of magnitude, the value of $D_{intra,tracer\text{-}desorption}$ is notably below these values. This finding has to be attributed to the influence of surface barriers which are known to occur quite commonly in LTA-type zeolites [39,49,50].

In Fig. 7 we have also displayed the diffusivities $D_{long\text{-}range} \equiv \langle r^2(t)\rangle_{long\text{-}range}/(6t)$ as resulting from the first, steep part of the signal attenuations (after subtraction of the slowly decaying, second part). Here we observed these high activation energies which one has to expect for long-range diffusion via the intercrystalline space. The deviation to smaller diffusivities as observed for the largest

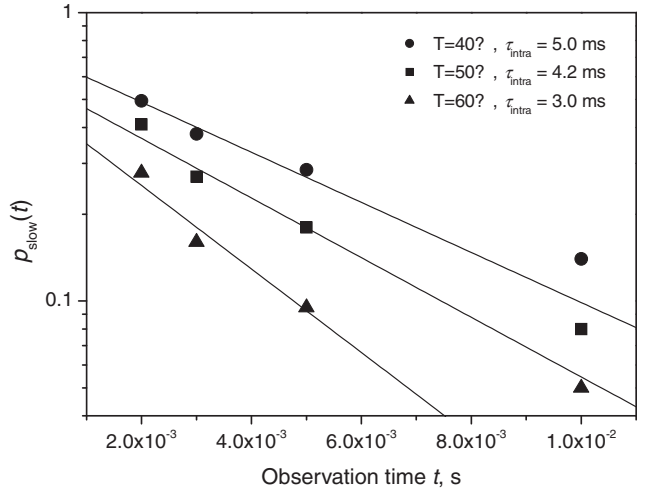

Fig. 6. Water diffusion in Na-LTA-2: The relative fraction $p(t)$ of the slowly decaying component of the PFG NMR spin-echo attenuation (see Fig. 5 for the representation at 50 °C) as a function of observation time t obtained at different temperatures 40 (circles), 50 (squares) and 60 °C (triangles). The lines show fits of the exponential function to the data at short times t with the time constants τ_{intra} indicated in the inset.

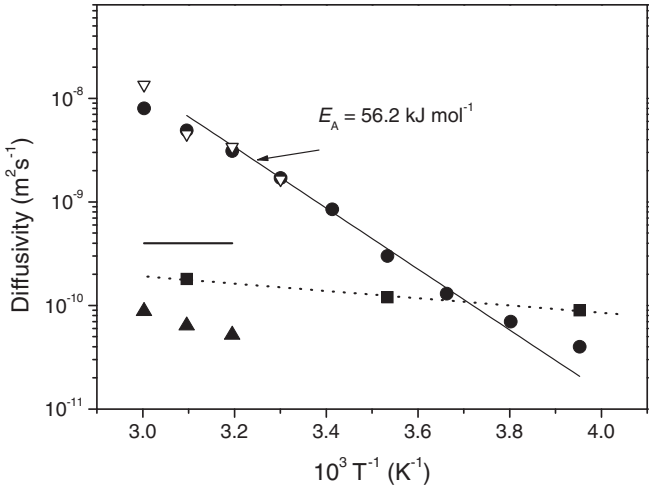

Fig. 7. Arrhenius plot of diffusivities of water in Na-LTA-2. The filled circles refer to long-range diffusivities ($D_{long\text{-}range}$), the filled triangles to diffusivities $D_{intra,tracer\text{-}desorption}$ estimated from tracer-desorption experiments. The horizontal line represents the value of $D_{restr.}$ following from Eq. (5) with $R = 2$ μm for an observation time $t = 2$ ms. For comparison, the literature data [39,43] on water diffusivity in Na-LTA-0 is shown by the filled squares. The open triangles show the long-range diffusivities for the sample Na-LTA-5.

temperatures reflects the transition from Knudsen to bulk diffusion in the intercrystalline space. It is brought about by the increasing gas phase concentration and, consequently, the increasing probability of mutual encounters of the gas molecules. Owing to the much larger distance in the intercrystalline pore space, this effect is expected to occur more pronounced in the beds of Na-LTA crystals than within the agglomerates of Na-BEA zeolite. It is interesting to note that there is also a perceptible deviation from the Arrhenius plot to larger values in the low-temperature range, i.e. in the limit of small displacements. With reference to the first term on the right-hand side of Eq. (10), this behaviour may be easily referred to the increasing contribution of intracrystalline displacements on the overall displacements (see, e.g., the detailed consideration of this phenomenon in [47]).

Most remarkably, these long-range diffusivities in beds of Na-LTA-2 are found to be nicely approached by the diffusivity data of water in Na-LTA-5. Having in mind that (i) the long-range diffusivity $D_{\text{long-range}} \equiv p_{\text{inter}} D_{\text{inter}}$ of the guest molecules is dominated by the conditions of the free space between the crystals, i.e. by the resulting diffusivities (D_{inter}) and the relative amounts of molecules (p_{inter}) and that (ii) these conditions may be expected to be similar to each other in Na-LTA-2 and Na-LTA-5, this agreement may be taken as a nice confirmation of our data interpretation. It is interesting to note that the more extensive mesopore network in the interior of Na-LTA-5, on the other hand, led to a notable acceleration of intracrystalline mass transfer and, equally important, to a reduction of transport resistances on the external surface of the individual crystallites so that molecular exchange between different crystallites became so fast that, even during the shortest observation times considered, essentially all guest molecules exchanged their positions between different crystals. This leads to the situation reflected by the dotted (straight) line in Fig. 5 (diffusion attenuation of water in Na-LTA-5): there is no perceptible fraction of molecules, anymore, which would remain within one and the same crystal (and would give rise, therefore, to the second, less steep decay, as observed with Na-LTA-2).

4. Conclusion

PFG NMR has been used for the exploration of mass transfer in mesoporous zeolites. With water as a probe molecule, over the space scale accessible in the PFG NMR measurements (0.6–10 μm) mass transfer in Na-BEA zeolite was found to follow normal diffusion, in accordance with Fick's 1st and 2nd laws. The considered displacements notably exceed the sizes of the individual particles. The measured diffusivities have to reflect, therefore, both the transport properties within the individual particles and the features of their interconnections within the agglomerates of Na-BEA zeolite. This transport mechanism deviates from the common type of mass transfer through beds of zeolite crystallites where mass transfer is dominated by diffusion through the intercrystalline space. It is thus only the influence of mesoporosity on the long-range diffusivities rather than on the intracrystalline diffusivities which are recorded by this type of experiments. It is interesting to note that, in comparison with Na-BEA-0 and Na-BEA-2, there is a pronounced increase in the long-range diffusivities of water in Na-BEA-5. Within the limits of the present study, however, it is impossible to unambiguously identify the origin of this finding.

The PFG NMR diffusion studies of water in mesoporous LTA zeolite reveal a totally different pattern. In the case of Na-LTA-2 zeolite, one may clearly distinguish between those molecules which, during the observation time, remain in one and the same crystal and those, which are able to exchange their positions between different crystals. Mass transfer of the latter fraction is expected to follow the mechanism of long-range diffusion. The large activation energies of the corresponding diffusivities confirm this assumption. The mean square displacement of those molecules which, during the observation time, did not leave the individual crystals may be notably exceeded by the displacements in an infinitely extended crystal. Hence, it is only possible to estimate a lower limit of the intracrystalline diffusivity. On the basis of this estimate, the mesoporosity is found to lead to both an increase in the intracrystalline diffusivities and a decrease in the transport resistances on the external surface of the zeolite crystallites.

Acknowledgements

Financial supports by the Ministry of Education, Science and Technology in Korea through the National Honor Scientist Program (20100029665) and World Class University Program (R31-2010-000-10071-0), and the Deutsche Forschungsgemeinschaft and the Fonds der ChemischenIndustrie in Germany are gratefully acknowledged.

References

[1] F. Schüth, K.S.W. Sing, J. Weitkamp, Handbook of Porous Solids, Wiley-VCH, Weinheim, 2002.
[2] R. Ryoo, S.H. Joo, J. Phys. Chem. B 103 (1999) 7743.
[3] M. Choi, H.S. Cho, R. Srivastava, C. Venkatesan, D.-H. Choi, R. Ryoo, Nat. Mater. 5 (2006) 718.
[4] M. Choi, R. Srivastava, R. Ryoo, Chem. Commun. (2006) 4380.
[5] G. Wang, E. Johannessen, C.R. Kleijn, S.W. de Leeuwa, M.O. Coppens, Chem. Eng. Sci. 62 (2007) 5110.
[6] O. Sel, M. Thommes, A. Brandt, D. Wallacher, B. Smarsly, Proceedings 19, Deutsche Zeolith-Tagung, Leipzig, 2007. p. 48.
[7] J.-H. Smatt, C. Weidenthaler, J.B. Rosenholm, M. Linden, Chem. Mater. 18 (2006) 1443.
[8] B.T. Holland, L. Abrams, A. Stein, J. Am. Chem. Soc. 121 (1999) 4308.
[9] C.J. Jacobsen, C. Madsen, J. Houzvicka, I. Schmidt, A. Carlsson, J. Am. Chem. Soc. 122 (2000) 7116.
[10] W. Fan, M.A. Snyder, S. Kumar, P.-S. Lee, W.C. Yoo, A.V. McCormick, R.L. Penn, A. Stein, M. Tsapatsis, Nat. Mater. 7 (2008) 984.
[11] H. Wang, T.J. Pinnavaia, Angew. Chem. Int. Ed. 45 (2006) 7603.
[12] D.P. Serrano, J. Aguado, J.M. Escola, J.M. Rodriguez, Á. Peral, Chem. Mater. 18 (2006) 2462.
[13] F.S. Xiao, L.F. Wang, C.Y. Yin, K.F. Lin, Y. Di, J.X. Li, R.R. Xu, D.S. Su, R. Schlogl, T. Yokoi, T. Tatsumi, Angew. Chem. Int. Ed. 45 (2006) 3090.
[14] A.H. Janssen, I. Schmidt, C.J.H. Jacobsen, A.J. Koster, K.P. de Jong, Micropor. Mesopor. Mater. 65 (2003) 59.
[15] M. Ogura, S.-Y. Shinomiya, J. Tateno, Y. Nara, E. Kikuchi, M. Matsukata, Chem. Lett. 29 (2000) 882.
[16] J.C. Groen, J.C. Jansen, J.A. Moulijin, J. Pérez-Ramírez, J. Phys. Chem. B 108 (2004) 13062.
[17] J.C. Groen, T. Bach, U. Ziese, A.M.P. van Donk, K.P. de Jong, J.A. Moulijin, J. Pérez-Ramírez, J. Am. Chem. Soc. 127 (2005) 10792.
[18] M. Choi, D.H. Lee, K.S. Na, B.W. Yu, R. Ryoo, Angew. Chem. Int. Ed. 48 (2009) 3673.
[19] K. Cho, H.S. Cho, L.C. de Menorval, R. Ryoo, Chem. Mater. 21 (2009) 5664.
[20] C.H. Christensen, K. Johannsen, E. Törnqvist, I. Schmidt, H. Topsøe, C.H. Christensen, Catal. Today 128 (2007) 117.
[21] J.C. Groen, W. Zhu, S. Brouwer, S.J. Huynink, F. Kapteijn, J.A. Moulijn, J. Pérez-Ramírez, J. Am. Chem. Soc. 129 (2007) 355.
[22] Y. Liu, W. Zhang, Z. Liu, S. Xu, Y. Wang, Z. Xie, X. Han, X. Bao, J. Phys. Chem. C 112 (2008) 15375.
[23] J. Kärger, H. Pfeifer, W. Heink, Adv. Magn. Reson. 12 (1988) 2.
[24] P.T. Callaghan, Principles of NMR Microscopy, Clarendon Press, Oxford, 1991.
[25] R. Kimmich, NMR Tomography, Diffusometry, Relaxometry, Springer, Berlin, 1997.
[26] R. Valiullin, J. Kärger, R. Gläser, Phys. Chem. Chem. Phys. 11 (2009) 2833.
[27] J. Kärger, in: H.G. Karge, J. Weitkamp (Eds.), Adsorption and Diffusion, Springer, Berlin, Heidelberg, 2008, pp. 85–133.
[28] J. Kärger, W. Heink, J. Magn. Reson. 51 (1983) 1.
[29] J. Kärger, Leipzig, Einstein, Diffusion, Leipziger Universitätsverlag, Leipzig, 2007.
[30] J. Kärger, AIChE J. 28 (1982) 417.
[31] R.M. Barrer, Zeolites and Clay Minerals as Sorbents and Molecular Sieves, Academic Press, London, 1978.
[32] P. Galvosas, F. Stallmach, G. Seiffert, J. Kärger, U. Kaess, G. Majer, J. Magn. Reson. 151 (2001) 260.
[33] F. Stallmach, P. Galvosas, Annu. Rep. NMR Spectr. 61 (2007) 51.
[34] K. Cho, R. Ryoo, S. Asahina, C. Xiao, M. Klingstedt, A. Umemura, M.W. Anderson, O. Terasaki, Solid State Sciences, in press. doi:10.1016/j.solidstatesciences.2010.04.22).
[35] D.W. Breck, Zeolite Molecular Sieves, Wiley and Sons, New York, 1974.

[36] J.O. Hirschfelder, C.F. Curtiss, R.B. Bird, Molecular Theory of Gases and Liquids, John Wiley & Sons, New York, 1964.
[37] A.J. Easteal, W.E. Price, L.A. Woolf, J. Chem. Soc. Faraday T. 1 (85) (1989) 1091.
[38] J. Kärger, Z. Phys. Chem. Leipzig 248 (1971) 27.
[39] J. Kärger, D.M. Ruthven, Diffusion in Zeolites and Other Microporous Solids, Wiley & Sons, New York, 1992. See also: J. Kärger, D.M. Ruthven, D.N. Theodorou, Diffusion in Zeolites and Other Nanoporous Materials, Wiley-VCH, Weinheim, 2011, in press.
[40] J. Kärger, P. Volkmer, J. Chem. Soc. Faraday Trans. I 76 (1980) 1562.
[41] H. Pfeifer, NMR Basic Princ. Prog. 7 (1972) 53.
[42] M. Dvoyashkin, A. Khokhlov, R. Valiullin, J. Kärger, J. Chem. Phys. 129 (2008).
[43] J. Kärger, H. Pfeifer, M. Rosemann, N.N. Feoktistova, S.P. Zdanov, Zeolites 9 (1989) 247.
[44] P.P. Mitra, P.N. Sen, L.M. Schwartz, P. LeDoussal, Phys. Rev. Lett. 68 (1992) 3555.
[45] P.P. Mitra, P.N. Sen, L.M. Schwartz, Phys. Rev. B 47 (1993) 8565.
[46] O. Geier, R.Q. Snurr, F. Stallmach, J. Kärger, J. Chem. Phys. 120 (2004) 1.
[47] J. Kärger, M. Kocirik, A. Zikanova, J. Colloid Interface Sci. 84 (1981) 240.
[48] J. Kärger, AIChE J. (1982) 417.
[49] J. Kärger, H. Pfeifer, R. Seidel, B. Staudte, T. Gross, Zeolites 7 (1987) 282.
[50] J. Kärger, H. Pfeifer, R. Richter, H. Furtig, W. Roscher, R. Seidel, AIChE J. 34 (1988) 1185.